Response of a Model Gas Turbine Combustor to Variation in Gaseous Fuel Composition

R. M. Flores
M. M. Miyasato
V. G. McDonell
G. S. Samuelsen[1]
e-mail: gss@uci.edu

UCI Combustion Laboratory,
University of California,
Irvine, CA 92697-3550

The effect of fuel composition on performance is evaluated on a model gas turbine combustor designed to mimic key features of practical devices. A flexible fuel injection system is utilized to control the placement of the fuel in the device to allow exploration and evaluation of fuel distribution effects in addition to chemistry effects. Gas blends reflecting the extremes in compositions found in the U.S. are considered. The results illustrate that, for the conditions and configuration studied, both fuel chemistry and fuel air mixing play a role in the performance of the device. While chemistry appears to be the predominant factor in stability, a role is noted in emissions performance as well. It is also found that changes in fuel distribution associated with changes in fuel momentum for fixed firing rate also have an impact on emissions. For the system considered, a strategy for sustaining optimal performance while fuel composition changes is illustrated.
[DOI: 10.1115/1.1377011]

Motivation

Gas turbines have been developed to operate on a wide variety of fuels and the significant role of the fuel composition in both operability and emissions have been noted (e.g., [1]). Lean-premixed combustion is increasingly becoming the method of choice for reducing pollutant emissions from natural gas-fired gas turbine power plants. However, as these systems operate closer to the edge of combustion stability to reduce emissions of NO_x, modest upsets in operating conditions, including those due to variation in fuel composition, are becoming intolerable.

Typical constituent concentrations for natural gas within the United States average 93.9 percent methane, with ethane, propane, and higher hydrocarbons rounding out much of the remaining composition at 3.2, 0.7, and 0.1 percent, respectively. However, methane, ethane, and propane compositions can approach values of 74.5, 13.3, and 23.7 percent, respectively ([2]).

This wide range of compositional variability in the U.S. natural gas supply poses a significant challenge for the development of combustors that can maintain optimal performance despite a wide range of natural gas compositions. As a result, a need for the systematic study of the effects of fuel composition on the performance of combustion systems is required. In addition, delineation of the key phenomena occurring is required in order to develop combustor designs that are insensitive to variations in fuel composition.

Objectives

The objectives of the current study are to (1) delineate the effects of fuel composition on the overall performance of a model combustor and (2) relate the variation in performance to fuel injection effects (i.e., mixing) and/or reaction characteristics (i.e., chemical kinetics).

Approach

The approach taken is to develop and apply a model combustor with characteristics similar to those found in practice. A flexible fuel injection system based on radial jets is employed in order to provide control over the fuel distribution entering the combustor. Performance maps based on CO, NO_x, and lean blow off (LBO) are generated as a function of fuel type and inlet fuel distribution. The fuel distribution is characterized at the inlet plane using an extractive probe to correlate the performance of the combustor.

Experiment

Test Facility. The test facility utilized provides a wide range of operating conditions and flow metering. The test stand is designed to operate at 1 atm with inlet temperatures up to 800 K. The model combustor test rig, shown in Fig. 1, is attached to a three-dimensional traverse system which allows the combustor to be moved as necessary to map out points both within and at the exit plane.

Model Combustor. The model combustor utilized is shown schematically in Fig. 2. Figure 3 shows the fuel injection options available. The fuel injection strategy involves a multipoint approach with the ability to control fuel flow splits between three independent fuel injection circuits. One available fuel injection option is to inject fuel radially from the centerbody into the swirl-

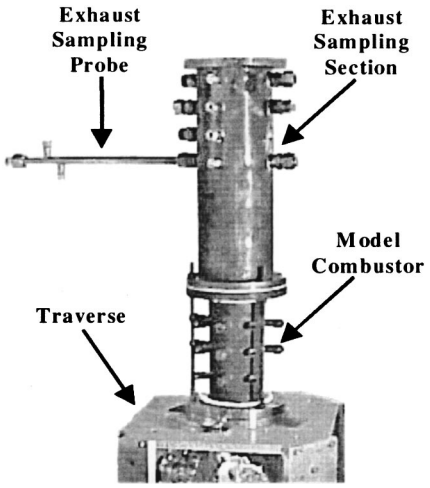

Fig. 1 Atmospheric test facility

[1]To whom correspondence should be addressed.

Contributed by the International Gas Turbine Institute (IGTI) of THE AMERICAN SOCIETY OF MECHANICAL ENGINEERS for publication in the ASME JOURNAL OF ENGINEERING FOR GAS TURBINES AND POWER. Paper presented at the International Gas Turbine and Aeroengine Congress and Exhibition, Munich, Germany, May 8–11, 2000; Paper 00-GT-141. Manuscript received by IGTI Oct. 1999; final revision received by ASME Headquarters Oct. 2000. Associate Editor: D. Wisler.

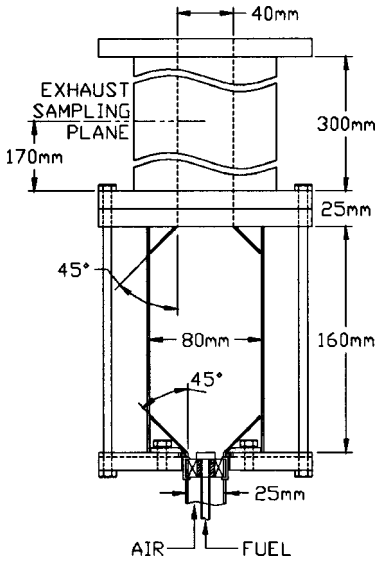

Fig. 2 Model combustor

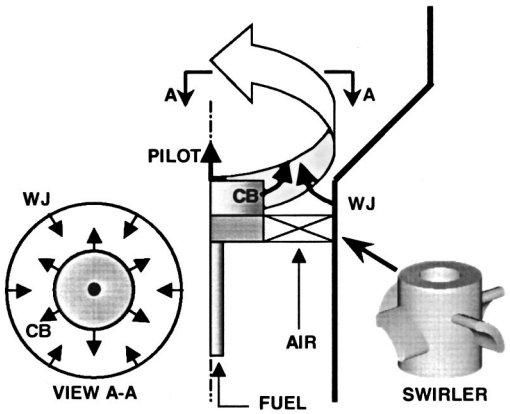

Fig. 3 Detail of fuel injection options

ing air stream. This centerbody injection circuit, labeled ''CB'' in Fig. 3, consists of six equally spaced fuel holes located circumferentially along the side of the fuel manifold. The fuel manifold is mounted to the centerbody tip, and is positioned directly against the swirler hub. The second fuel injection option is to inject the fuel radially from the surrounding wall. This wall injection circuit, labeled ''WJ'' in Fig. 3, consists of six equally spaced fuel holes in positions that are staggered with respect to the centerbody injection holes. The final fuel injection option is to inject the fuel axially into the air stream. This axial injection circuit, labeled ''PILOT'' in Fig. 3, consists of a single fuel injection hole located at the tip of the centerbody.

The baseline configuration is a four vane axial swirler. The nominal firing rate for the system is 15 kW at 0.0093 kg/sec of air, though the fuel flow rates were varied to assess the system's performance. An air inlet temperature of 700 K was utilized in all cases.

Diagnostics. Exhaust emissions of carbon monoxide (CO), carbon dioxide (CO_2), hydrocarbons (HC), oxygen (O_2), and nitrogen oxides (NO_x) were measured using Horiba Ltd, analyzers. These instruments are part of an integrated sampling and computer data acquisition system.

A 12.7-mm o.d. water-cooled, stainless steel bulk emissions probe is used to sample the exhaust emissions downstream of the exit plane of the combustor as shown in Fig. 1. This probe is designed to take an integrated average measurement of the emissions over the diameter of the sampling plane. The water in the probe is heated to 325 K to protect the probe and quench the sample while avoiding condensation of water vapor in the sample. The emissions are pumped through a Teflon line heated to 408 K to prevent water condensation, and the sample is then split into two streams. The NO_x stream goes through a converter to reduce any NO_2 to NO prior to the water drop out.

All of the emissions measurements from the analyzers are recorded using a digital data acquisition system. The measurements from the analyzers are sampled over a 20 second period at a rate of 5 Hz. One hundred samples from each analyzer are averaged and recorded in a data file. The residence time associated with the gases flowing through the combustor and to the exhaust sample probe is 24.8 msec. The reference velocity (based on nonreacting, nonpreheated conditions) for the model combustor is 1.55 m/s.

The nonreacting fuel distribution at the swirler exit was mapped with a 12.7 mm o.d. stainless steel probe and a high range flame ionization detector (Horiba Model FIA-236-1).

Fuel Blending. For the current study, a subset of a comprehensive fuel blending system was utilized as illustrated in Fig. 4. Natural gas, ethane, and propane can be combined in any desired combination using this system. A series of Brooks mass flow controllers are utilized in conjunction with a LabView based control program which allows the user to set fuel composition and flow splits as desired. The overall accuracy of the blended fuel flow rate is ± 2 percent.

Noteworthy is the use of natural gas as a baseline fuel. In order to account for any compositional variations in the natural gas, a dedicated on-line gas composition analyzer is utilized to provide baseline concentrations.

Table 1 summarizes the typical natural gas composition utilized. Fortunately, methane comprises the vast majority of the natural gas. As a result, by studying the effect of adding 15 per-

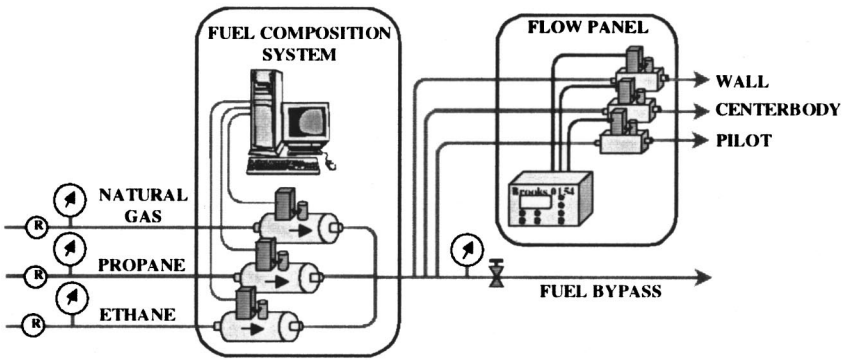

Fig. 4 Fuel blending system

Table 1 UCICL natural gas composition

n	Constituent		MF $y(i)$percent
1	Methane	CH_4	96.975
2	Ethane	C_2H_6	0.982
3	Propane	C_3H_8	0.109
4	iso-Butane	C_4H_{10}	0.014
5	n-Butane	C_4H_{10}	0.015
6	iso-Pentane	C_5H_{12}	0.004
7	n-Pentane	C_5H_{12}	0.004
8	C6	C_6H_{14}	0.001
9	C7	C_7H_{16}	0.001
10	C8	C_8H_{18}	0.000
11	CO_2		1.574
12	O_2		0.000
13	N_2		0.322
		Totals	100.00

Table 2 Gas compositions utilized

Blend	Wobbe Index* MJ/m^3	S.G. relative to air	LHV MJ/m^3
Natural Gas	44.3	0.576	33.6
85 percent Natural Gas/ 15 percent Ethane	46.8	0.645	37.6
80 percent Natural Gas/ 20 percent Propane	50.5	0.765	44.2
Propane	70.1	1.523	86.5

*Wobbe Index=LHV/$[SG]^{1/2}$ ([1])

cent ethane or 20 percent propane by volume, the effects of the minor constituents present in the baseline natural gas are felt to carry a negligible effect relative to the results obtained.

For the present study, four fuel compositions were considered. Some of the associated properties are summarized in Table 2.

Results

Overall combustion performance is first summarized, followed by correlations with fuel distribution, and finally, fuel injection mechanisms. The combustor performance is based on the lean blow off (LBO) limits and the emissions of CO and NO_x, both of which are corrected to a fixed dilution of 15 percent O_2. In the current system, the LBO limit will depend upon both the mixing and reaction rates. As fuel composition changes, the reaction rate will change. An increased reaction rate will help extend the LBO limits. However, since a radial fuel injection strategy is utilized, and the fuel distribution depends upon the momentum ratio of the fuel jet to the swirling air, the fuel composition can also affect the jet behavior and the subsequent mixing. In addition, the NO_x levels will depend not only the local reaction temperature, which can be a function of fuel composition, but also upon differing NO_x formation mechanisms (e.g., [3,4]).

Combustor Performance

Emissions. The combustion performance for each fuel mixture was assessed via maps of NO_x and CO emissions, corrected to 15 percent O_2, as a function of injector fuel split (relative to the Pilot, Wall Jet, and/or Centerbody injectors). Figure 5 summarizes the results obtained for 100 percent natural gas with and without pilot fuel. The white regions on the lean side of each plot reflect regions beyond the LBO limits. Results are shown for NO_x emissions (Figs. 5(*a*) and 5(*c*)) and the corresponding CO emissions (Figs. 5(*b*) and 5(*d*)) as a function of overall equivalence ratio and percentage of fuel injected radially outwards from the centerbody (recall Fig. 3). Note that the fuel split between the centerbody and wall injectors is of the remaining fuel *after* the pilot fuel (if any) is subtracted. The results illustrate several key features. First, for the cases without pilot fuel (Figs. 5(*a*) and 5(*b*)), the NO_x levels appear relatively insensitive to fuel split (percent Centerbody), while revealing typical dependency upon reaction temperature (Eq. Ratio). CO emissions reveal a ''u-shaped'' profile with an increase in CO under extremely lean conditions and at equivalence ratios greater than 0.47.

Figures 5(*c*) and 5(*d*) illustrate that the pilot fuel has a significant impact on the performance. Although the LBO limits are extended from $\phi=0.38$ to $\phi=0.32$, high amounts of CO and NO_x are emitted. Since the pilot fuel is injected axially into the central recirculation zone, a rich, high-temperature core with limited mixing must result to give rise to the higher NO_x *and* CO. As such, the extension of the LBO limit is handicapped by increased emissions.

As shown in Fig. 5, CO and NO_x emission levels often move in opposite directions. As a result, it is important to identify conditions and configurations that minimize both. This can be achieved by utilizing a ''performance function.'' J:

$$J = w_{\eta c} \cdot J_{\eta c} + w_{\mathrm{NO_x}} \cdot J_{\mathrm{NO_x}} \tag{1}$$

where η_c is the combustion efficiency, which is a function of CO and unburned hydrocarbon (HC) emissions, and the terms $w_{\eta c}$ and $w_{\mathrm{NO_x}}$ are weighting factors whose sum is equal to one. For this study, since HCs were zero for essentially all cases, the η_c represents a normalized function of CO emissions. The functions $J_{\eta c}$ and $J_{\mathrm{NO_x}}$ are defined as

$$J_{\mathrm{NO_x}} = \begin{cases} 1 - 0.75 \cdot \left(\dfrac{[\mathrm{NO_x}]}{5} \right)^4, & [\mathrm{NO_x}] \leqslant 5 \text{ ppm} \\ (1-0.75) \cdot \dfrac{[\mathrm{NO_x}]_{\mathrm{MAX}} - [\mathrm{NO_x}]}{[\mathrm{NO_x}]_{\mathrm{MAX}} - 5}, & [\mathrm{NO_x}] > 5 \text{ ppm} \end{cases}$$

$$J_{\eta c} = \begin{cases} 0, & \eta < 99.98 \text{ percent} \\ \left(\dfrac{\eta - \eta_{\mathrm{MIN}}}{100 \text{ percent} - \eta_{\mathrm{MIN}}} \right)^{1/2}, & \eta \geqslant 99.98 \text{ percent.} \end{cases}$$

The functions $J_{\eta c}$ and $J_{\mathrm{NO_x}}$ were selected to yield high values of J when the combustion efficiency is high (low CO) and the NO_x is low. From the definitions of $J_{\eta c}$ and $J_{\mathrm{NO_x}}$, the values of J that may be obtained range from a minimum of zero, signifying poor performance, to a maximum of one, indicating ideal performance. For the results presented here, $w_{\eta c}$ and $w_{\mathrm{NO_x}}$ are equally weighted at 0.5.

With this combined CO and NO_x function, the areas on the map with optimal performance (or nonoptimal performance) can be identified and the extent to which fuel composition alters the regions of optimal performance noted.

Figure 6 shows the results from Fig. 5, presented in terms of the performance index J, with the results for three other fuel compositions. Figure 6 illustrates the utility of combining the NO_x and CO performance into a single quantity in order to evaluate operational trends. The pilot fuel has a major impact on performance for the conditions selected, and a distinct maximum in performance is observed for cases without pilot. The response appears as a ridge associated with a fairly broad range of equivalence ratios. However, the ridge has a peak which is a function of the fuel splits.

As a result, it can be seen that the fuel composition has an impact on the optimal fuel injection strategy for the conditions under considerations in this study.

To help provide additional insight into the behavior, some specific conditions were identified for further analysis. These cases are indicated on Fig. 6. One set reflects a fixed equivalence ratio

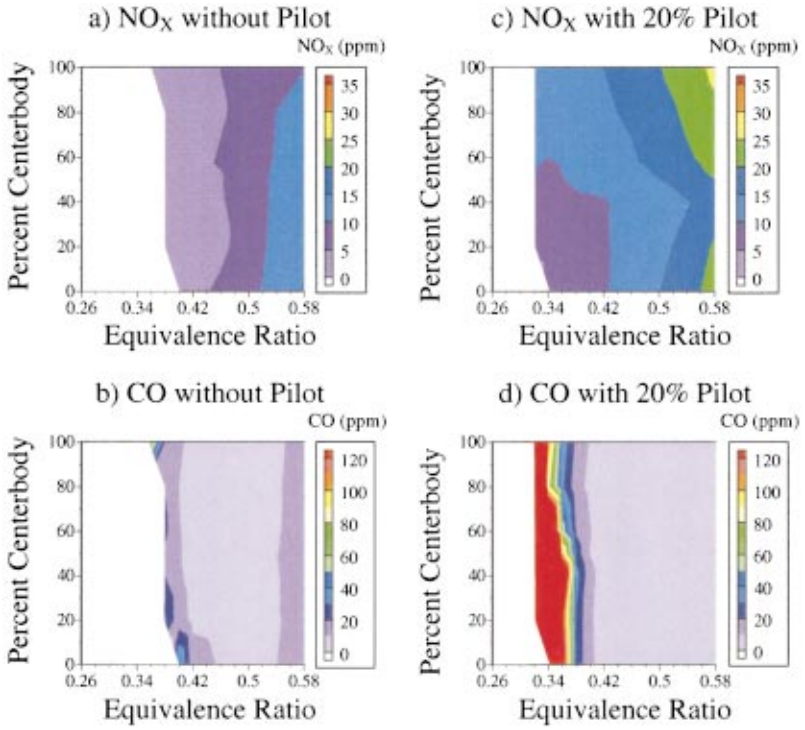

Fig. 5 Emission levels for 100 percent natural gas

and fixed fuel injection strategy to isolate the effect of fuel composition (cases 1–4). The other set reflects the optimal performance for each fuel composition (cases 5–7).

The isolated effect of fuel composition is summarized in Table 2 for an equivalence ratio of 0.42 and a fuel split of 80 percent centerbody—20 percent wall with no pilot fuel. These results show that, compared to 100 percent natural gas, CO levels decreased, while NO_x levels increased. Part of this behavior may be explained by the calculated reaction temperatures, which are also included in Table 3 for a fully premixed case.

Table 3 illustrates two key points. First, the average premixed temperatures are well below the threshold for NO_x formation (i.e., 1900 K). This means that, for the appreciable NO_x levels measured, local regions with higher temperatures (i.e., equivalence

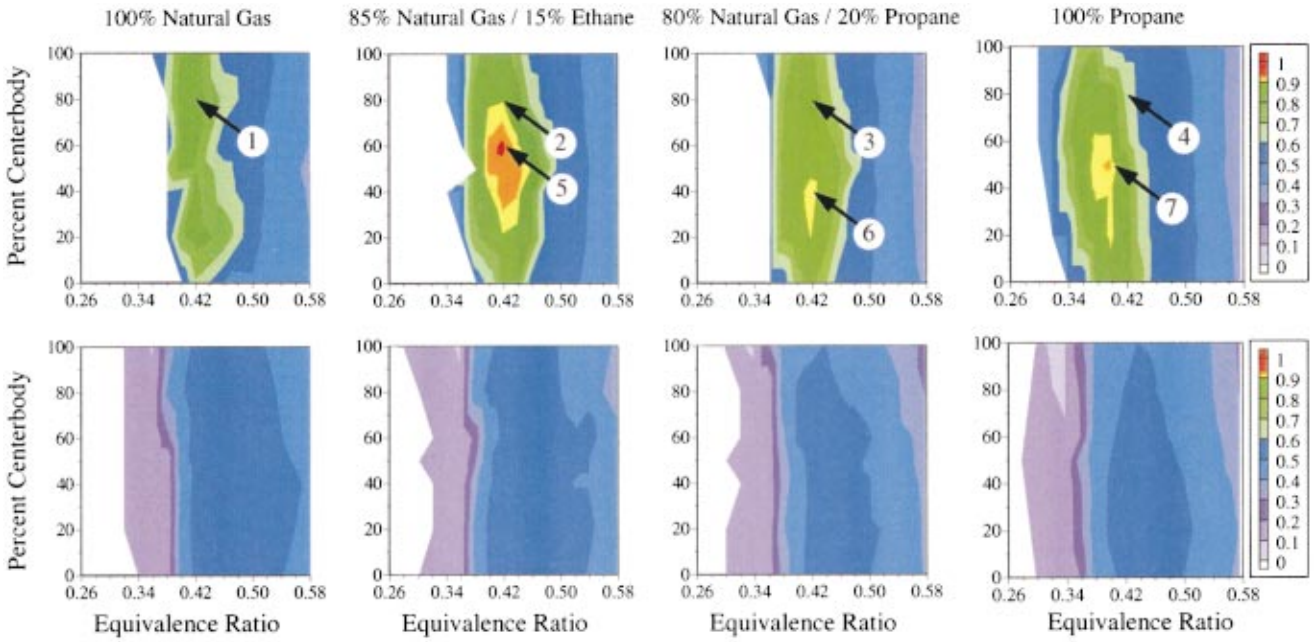

Fig. 6 Performance function for fuel composition (top: no pilot fuel; bottom: 20 percent pilot fuel)

Table 3 Relative emissions and calculated temperatures versus fuel composition for fixed equivalence ratio (ϕ=0.42) and fuel split

Case	$CO/CO_{nat\ gas}$	$NO_x/NO_{x\ nat\ gas}$	Tad*, K
85 percent nat gas 15 percent ethane (Case 2)	0.54	1.25	1616
80 percent nat gas 20 percent propane (Case 3)	0.86	1.25	1620
100 percent propane (Case 4)	0.55	1.87	1637

*Tadiabatic for Case 1: 1612 K

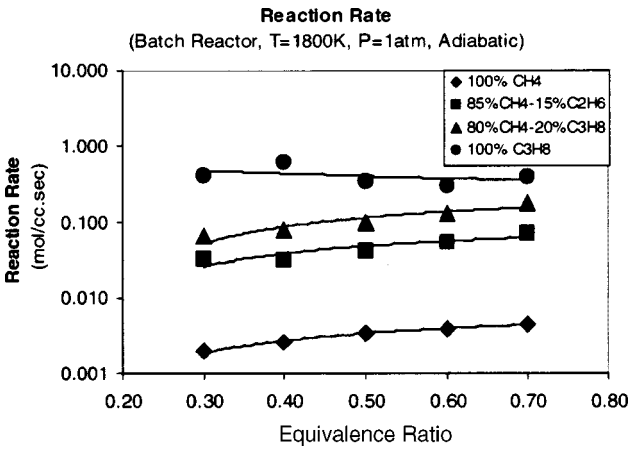

Fig. 7 Calculated reaction rates for methane—85 percent methane–15 percent ethane, and 80 percent methane–20 percent propane ([8])

ratios) must be present if thermal NO_x is contributing. The results also illustrate that the peak temperatures will be higher for the fuels other than ''pure'' natural gas, thus providing one reason for the increased NO_x levels in these cases. The increased reaction temperatures may also lead to faster oxidation of CO. What is not revealed in Table 3 is the relative contribution of nonthermal NO_x mechanisms (e.g., N_2O pathway) which can also depend upon fuel type ([4]). For the conditions considered, it has been suggested that both mechanisms are important ([3]).

Lean Blow-Off Limits. The fuel composition and fuel injection strategy also have an impact on the LBO limits. ''Pure'' natural gas has the richest, LBO limit while the 100 percent propane case has the widest LBO range. Without pilot fuel, a slight trend of improved LBO limits with increased centerbody fuel injection is indicated.

With pilot fuel, the LBO range is broadened, but the overall performance is systematically worse compared to the cases with no pilot fuel. The reason for this degraded performance is attributed to higher emissions of both CO and NO_x, as illustrated in Fig. 5.

That the pilot fuel extends the LBO limits is not surprising and is, in fact, expected. The pilot fuel enriches the recirculation zone and thereby extends the limits. However, the improved LBO limits is accompanied by a degradation in performance (Fig. 6). Because the amount of fuel utilized may play a role, additional tests were conducted with 10 percent pilot fuel. These tests revealed similar trends. Consideration has not yet been given to the use of a more energetic fuel (e.g., H_2 addition—([5])) but remains the topic of future planned work.

In the case without pilot fuel, the fuel composition itself impacts the LBO limits in a manner consistent with reaction rates. Figure 7 illustrates this factor by comparing the calculated relative reaction rates of 100 percent methane, a mixture of 85 percent methane and 15 percent ethane, and a mixture of 80 percent methane and 20 percent propane. These amounts of ethane and propane lead to reaction rates that are a factor of ten or more faster. This, of course, is one reason why long premixing times can lead to problems with auto-ignition when fuel compositions vary. Recent work has illustrated a correlation of LBO limits with Peclet number, which is based in part on the kinetics of the process (e.g., [6]). This appears to be the case in the present study as well. With pilot fuel, less variation in LBO limits are noted, suggesting a different stabilizing mechanism in this case (e.g., since the fuel is injected directly into the reaction zone, a more ''diffusion-type'' reaction is present).

Fuel Distribution. Based on the emissions results, the chemistry of the process appears to be the primary reason for the variation in LBO. However, the relative contribution of fuel distribution must also be assessed to substantiate this conclusion.

The above measurements were taken at a fixed air flow (i.e., combustor pressure drop) while matching the firing rates for each fuel (equivalence ratios). Due to the difference in the heat content of the fuels, the gas volume flow rates also varied substantially. As a result, it might be expected that the fuel distributions will vary depending upon the gas blend. To start assessing this issue, calculations were done based on an empirical expression for a jet injected into a cross flow for the different fuels ([7])

$$x = D_{\text{jet}} \cdot q^{0.425} \cdot \left(\frac{y}{D_{\text{jet}}} \right)^{0.38} \tag{2}$$

where

$$q = \frac{\rho_{\text{jet}} \cdot V_{\text{jet}}^2}{\rho_{\text{air}} \cdot V_{\text{air}}^2}$$

Figure 8 shows the results for natural gas and propane for a fixed firing rate of 12.7 kW at a constant crossflow velocity. The results illustrate that the natural gas fuel jet penetration is limited to substantially less than half the annulus by the time it reaches the reaction zone; and accordingly, the propane jet penetration is 50 percent less (corresponding to a 2.5 flow rate ratio). These results illustrate the potential for fuel composition to play a role in the spatial distribution of the fuel.

To add to the understanding of the fuel distribution effects on performance, the spatial distribution of fuel entering the combus-

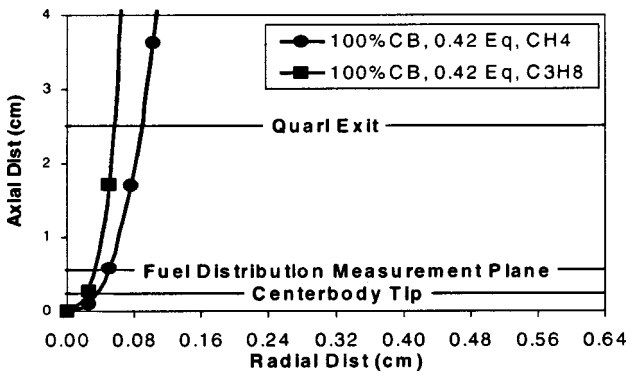

Fig. 8 Relative penetration of natural gas and propane at fixed firing rates for centerbody injection, wall jet injection, and a 50 percent split

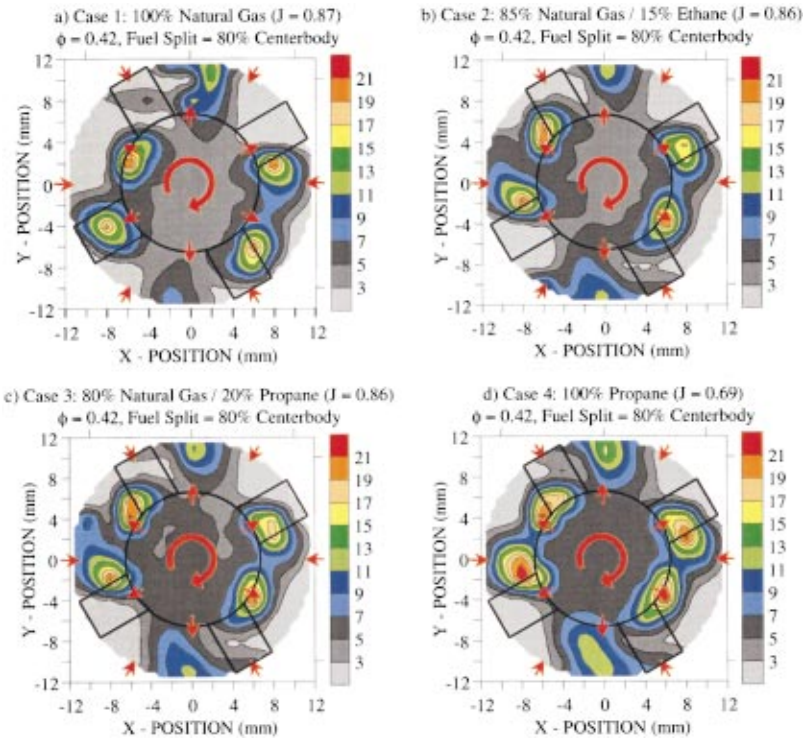

Fig. 9 Fuel distributions for cases 1–4 in Fig. 6 (concentrations presented in equivalent C atoms)

tor was measured for the seven cases which are numbered on Fig. 6. Nonreacting hydrocarbon measurements were conducted at a plane 3 mm downstream of the centerbody face. The results for the seven cases are shown in Figs. 9 and 10. The arrows indicate the direction and location of the fuel jets, with the swirl direction indicated by the counterclockwise arrow; the location of the four swirl vanes are also represented as the open boxes.

The results illustrate several key points. First, the distinct fuel jets are evidenced by the high fuel concentrations near the centerbody and wall jet injection locations. The six discrete centerbody injection points are easily distinguished in the results, suggesting that the fuel is not well mixed at the combustor inlet.

The results also reveal a distinct asymmetry in the jets, especially the jets at the ''12 o'clock'' and ''6 o'clock'' positions. Closer assessment of the geometry reveals the reason for the variation in the jet behavior. The alignment of the jets and vanes lead to three different patterns (with a symmetry plane consisting of a 180 deg sector). The position of the jet relative to vane plays a key role in the mixing. The 12 o'clock and 6 o'clock jets are oriented at the same location, as are the 1:30 and 7:30 and 4:30 and 10:30 pairs. Depending upon the location of these pairs relative to the position of the swirler vanes, the mixing varies considerably.

Considering the analysis from Fig. 8, it is anticipated that the propane would penetrate much less than the natural gas. However, for the results presented, the jet is heavily underpenetrating for either propane or natural gas. As a result, at the measurement plane shown in Fig. 8, differences may be difficult to resolve.

Indeed, based on the measured fuel distribution shown in Fig. 9, no clear differences are noticed as a function of fuel distribution for the same equivalence ratio (0.42), despite a large change in performance between cases 1 and 4. Since the distribution remains similar for the different fuel compositions, the changes in performance are attributed primarily to chemistry at the given equivalence ratio and fuel split.

To further explore the role of fuel distribution, Fig. 10 presents the distributions for cases 1 and 5–7. These cases represent the optimal performance cases for each fuel blend. For these four cases, the NO_x and CO levels are comparable. When comparing the optimal cases, significant differences are exhibited compared to those in Fig. 9 (Figs. 9(*a*) and 10(*a*) are the same). The results displayed in Fig. 10 show a more uniform fuel distribution at the optimal conditions compared to the corresponding nonoptimal conditions shown in Fig. 9 (e.g., cases 4 versus 7, 3 versus 6, 2 versus 5). This suggests that fuel distribution does play a role in the performance in addition to the chemistry and that different fuel blends require different optimization conditions. To help quantify the differences, Table 4 shows the relative variation in fuel distribution for each case with the relative performance. Some trend with improved mixing (i.e., reduced normalized rms) is noted, for a given fuel composition (e.g., cases 4 versus 7, 3 versus 6, 2 versus 5).

Fully Premixed Studies. To further isolate the effects of chemistry from mixing, a study was conducted using fully premixed conditions. This was achieved by injecting the fuel well upstream of the inlet to the combustor and measuring the exhaust emissions at various equivalence ratios up to LBO limit. The fully premixed condition was verified using the setup used to measure the fuel distributions shown in Figs. 9 and 10.

The NO_x and CO emissions results from this study are shown in Figs. 11 and 12 in terms of calculated adiabatic flame temperature based on the equivalence ratio. A dependency of the lean blow off limit with fuel composition is illustrated (most clearly shown in Fig. 12). The trends are consistent with the observations based on the kinetics calculations (Fig. 7). The results also illustrate that the fuel composition plays a role in the emissions performance at temperatures above 1750 K. Propane generates more NO_x than natural gas at the same reaction temperature. This is attributed to the role of the nonthermal NO_x mechanisms that are impacted by fuel composition, including prompt NO_x and N_2O pathways. Finally, comparing the results from Fig. 11 to those in Fig. 5 indicates that the current system could achieve somewhat lower NO_x levels with improved mixing. However, the requirements of turn-

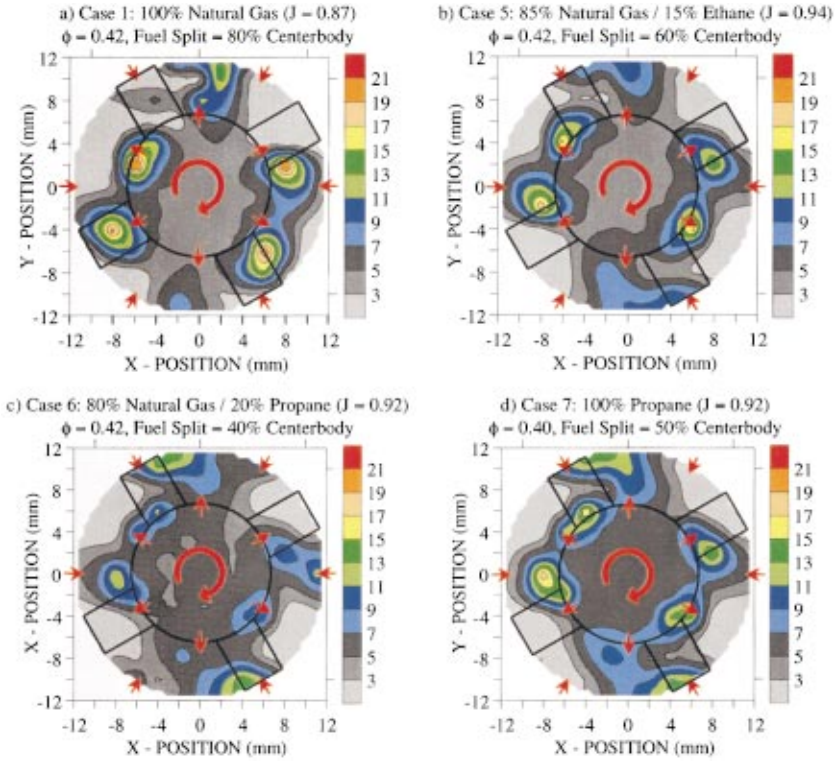

Fig. 10 Fuel distributions for optimal fuel injection strategies (cases 1, 5, 7) (coordinates are shown in millimeters and concentrations are presented in equivalent C atoms)

down, avoidance of flashback and autoignition, and robustness to fuel composition variability make a completely premixed system less attractive than the controlled lean rapid mix injection strategy utilized in the present study.

Summary and Conclusions

The results presented illustrate the role of fuel composition on the performance and fuel distribution in a model gas turbine combustor with controllable fuel injection strategies. The combustion performance in the present case is based on emissions of CO and NO_x, which are combined into a performance function, and the lean blow off limits.

The results indicate that:

- Changes in lean blow-off limits correlate with reaction rate, suggesting that a kinetic mechanism is responsible for stabilizing the reaction in the present case. This is reaffirmed by studies using fully premixed conditions.
- The measured fuel distributions for fixed operating conditions reveal little dependency upon fuel composition despite significantly varying momentum flux ratios. This is attributed to the

Table 4 Spatial variation versus fuel type and condition

Case	J, Performance	Rms Fuel Concentration/Mean Fuel Concentration
1	0.87	0.83
2	0.90	0.77
5	0.94	0.68
3	0.87	0.78
6	0.92	0.61
4	0.69	0.75
7	0.92	0.65

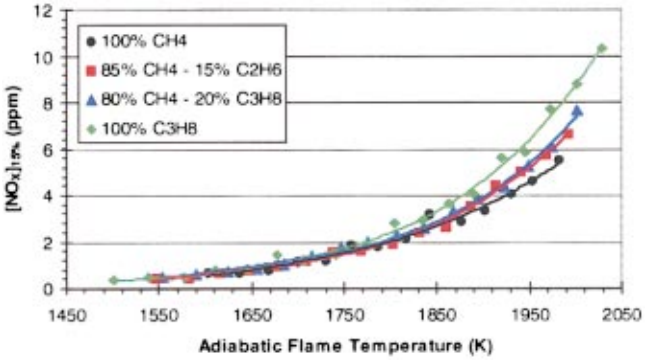

Fig. 11 NO_x concentrations for fully premixed cases

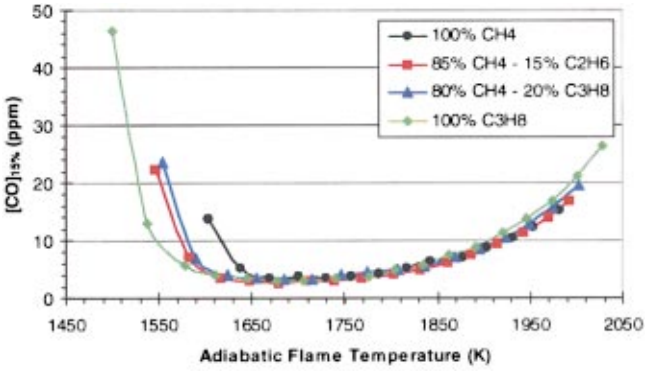

Fig. 12 CO concentrations for fully premixed cases

relatively weak penetration of the fuel jets in each case. This may be a strategy to minimize sensitivity of the mixing to fuel compositional changes.

• The fuel composition plays a role in NO_x emissions, with higher hydrocarbons generating more NO_x for a given firing temperature, independent of differences in mixing. This is attributed to the participation of nonthermal NO_x formation pathways that depend upon fuel composition.

• With the adaptive fuel injection strategy utilized in the present study, it is possible to compensate for fuel composition changes and maintain combustion performance at an optimal level. This is likely to have even more utility as load changes in addition to fuel composition.

Acknowledgments

The authors acknowledge the support of the US Department of Energy Advance Turbine Systems program and the South Carolina Institute for Energy Studies (SCIES). The contributions of Mr. Mark Vardakas, Mr. Junhua Chen, and Mr. Steve Hill are gratefully appreciated.

References

[1] Meier, J. G., Hung, W. S. Y., and Sood, V. M., 1986, ''Development and Application of Industrial Gas Turbines for Medium-BTU Gaseous Fuels,'' ASME J. Eng. Gas Turbines Power, **108**, pp. 182–190.

[2] Liss, W. E., Thrasher, W. H., Steinmetz, G. F., Chowdiah, P., and Attari, A., 1992, ''Variability of Natural Gas Composition in Select Major Metropolitan Areas of the United States,'' GRI-92/0123 Mar.

[3] Nicol, D. G., Steele, R. C., Marinov, N. M., and Malte, P. C., 1995, ''The Importance of the Nitrous Oxide Pathway to NO_x in Lean-Premixed Combustion,'' ASME J. Eng. Gas Turbines Power, **117**, pp. 100–111.

[4] Steele, R. C., Jarrett, A. C., Malte, P. C., Tonouchi, J. H., and Nicol, D. G., 1997, ''Variables Affecting NO_x Formation in Lean-Premixed Combustion,'' ASME J. Eng. Gas Turbines Power, **119**, pp. 102–107.

[5] Nguyen, O. M., and Samuelsen, G. S., 1999, ''The Effect of Discrete Pilot Hydrogen Dopant Injection on the Lean Blowout Performance of a Model Gas Turbine Combustor,'' ASME Paper No. 99-GT-359.

[6] Hoffmann, S., Lenze, B., and Eickoff, H., 1998, ''Results of Experiments and Models for Predicting Stability Limits of Turbulent Swirling Flames,'' ASME J. Eng. Gas Turbines Power, **120**, pp. 311–316.

[7] Beer, J. M., and Chigier, N. A., 1972, Combustion Aerodynamics, Robert E. Krieger Publishing Co., Malabar, FL.

[8] Kee, R. J., et al., 1999, *Chemkin Collection, Release 3.5*, Reaction Design, San Diego, CA.